

Original Article

Electroacupuncture improves lipid metabolism via proteome and gut microbiota profiling in obese rats

Xia Liu^{1*}, Chang She^{2*}, Xiang Li¹, Menglin Yang¹, Yunhui Zhang¹, Penglong Yu¹, Yanqiu Tong^{3,4}, Xunhao Zhang¹, Xiurong Tian^{1,5}

¹School of Traditional Chinese Medicine, Chongqing Three Gorges Medical College, Chongqing 404120, China;

²Department of Acupuncture and Moxibustion Rehabilitation, Changsha Hospital of Traditional Chinese Medicine (Changsha Eight Hospital), Changsha 410100, Hunan, China; ³College of Basic Medicine, Chongqing Medical University, Chongqing 400016, China; ⁴School of Tourism and Media, Chongqing Jiaotong University, Chongqing 400074, China; ⁵First Clinical College, Shandong University of Traditional Chinese Medicine, Jinan 250355, Shandong, China. *Equal contributors.

Received November 26, 2024; Accepted May 11, 2025; Epub May 15, 2025; Published May 30, 2025

Abstract: Objectives: Electroacupuncture (EA) is widely utilized for obesity treatment, but the mechanisms remain incompletely understood. This study explored electroacupuncture effects on gut microbiota and adipose tissue proteomics in obese rats. Methods: Twenty-two Sprague-Dawley male rats were randomly divided into the control (n=6) and model (n=16) groups. After establishing an obesity model, the rats were further categorized into the high-fat diet (n=6) and EA groups (n=6). The EA group underwent EA at “Quchi” (LI 11) and “Zusanli” (ST 36) acupoints for 21 days. Body weight was measured on alternate days, and hematoxylin and eosin staining were used to assess pathological changes in the adipose tissue and liver. Serum lipid levels were measured using a biochemical analyzer. Amplicon sequencing for bacterial 16S rRNA gene and liquid chromatography-mass spectrometry determined the gut microbiota structure and short-chain fatty acid (SCFA) content in the fecal sample, respectively. Tandem mass tag quantitative proteomics was used to analyze differentially expressed adipose tissue proteins. Results: EA significantly reduced body weight, improved adipose tissue pathology, and decreased total cholesterol and triglyceride levels. EA significantly modulated key gut microbiota involved in lipid metabolism and increased SCFA content, particularly acetic and propionic acids. The proteomic analysis revealed EA-mediated protein regulation, including Hmgcs1 (3-Hydroxy-3-Methylglutaryl-CoA Synthase 1) and Fabp3 (Fatty Acid-Binding Protein 3), associated with peroxisome proliferator-activated receptor (PPAR) signaling pathway regulation. Conclusion: EA improved dysregulated gut microbiota and SCFAs, modulated PPAR signaling, and improved lipid metabolism; thus, it has a potential role in obesity treatment.

Keywords: Electroacupuncture, obesity, gut microbiota, PPAR signaling pathway

Introduction

Recently, the prevalence of obesity has escalated worldwide, reaching pandemic levels [1], with projections estimating that by 2030, 38% of the global population will be overweight and 20% will be classified as obese [2]. Obesity is strongly correlated with chronic conditions, including cardiovascular diseases, type 2 diabetes, hypertension, and osteoarthritis. Additionally, individuals with obesity frequently grapple with psychological issues such as anxiety, depression, and diminished self-esteem, which significantly impact social interactions [3-5].

Treatment modalities for obesity include dietary interventions, exercise, pharmacotherapy, and surgical procedures [6]; however, adherence to dietary restrictions and exercise regimens often prove challenging. In contrast, drug therapies have potential side effects, including diarrhea, drowsiness, irregular heart rate, and harm to the liver and kidneys [3, 7]. Although surgical interventions can yield substantial weight loss, they also pose complications such as gastric acid reflux, malnutrition, and bleeding [8, 9]. Hence, there is an urgent need to identify suitable approaches to tackle obesity. Electroacupuncture (EA), an integral compo-

EA improves lipid metabolism

ment of traditional Chinese medicine, is a promising weight loss modality due to its simplicity, convenience, effectiveness, and low cost [10]. Widely applied in clinical practice, EA has proven its therapeutic potential [11, 12]. Nevertheless, the exact mechanisms underlying its health-beneficial effects remain poorly understood.

The gut microbiota greatly impacts the initiation and progression of obesity. In 2005, a research team discovered that the gut microbiota of patients with obesity exhibited an imbalance, characterized by a notable increase in the Firmicutes/Bacteroidetes ratio [13]. Short-chain fatty acids (SCFAs) are metabolites of the gut microbiota [14] and have regulatory effects on energy metabolism and supply. Recently, acupuncture and moxibustion have gained widespread acceptance in obesity management. Our previous research has demonstrated that EA reduces weight, with its mechanism closely related to the hypothalamic regulation of food intake [15]. Several studies have suggested that EA may regulate the abundance of gut microbiota in obese rats [16]; however, further investigations are needed to explain the exact process of EA influence on gut microbiota, particularly its potential relationship with metabolites such as SCFAs. Proteomics is a burgeoning field that delves into the composition and alterations of all proteins within a species, individual, organ, tissue, or cell genome [17, 18]. The holistic approach of traditional Chinese medicine aligns seamlessly with the emphasis on integrity and thoroughness in proteomics [19].

This study investigated the effect of EA on the gut microbiota and its corresponding metabolites, specifically SCFAs, in simple obese rats. Proteomic techniques were employed to screen for differentially expressed proteins (DEPs) in the adipose tissue of simple obese rats following EA intervention to elucidate the underlying mechanism of EA treatment for obesity.

Materials and methods

Animals

Twenty-two Sprague-Dawley rats (males, 4 weeks old, 150 ± 10 g) were acquired from Hunan SJA Laboratory Animal Co., Ltd. (Changsha, China). This animal experiment

received approval from the Biomedical Ethics Committee of Chongqing Three Gorges Medical College (ethical review approval number: SYYZ-A-2211-0001). All experimental procedures were conducted in accordance with the National Institutes of Health (NIH) Guide for the Care and Use of Experimental Animals (National Academies Press, Bethesda, MD, USA).

The rats were kept at the Experimental Animal Center of Chongqing Three Gorges Medical College under controlled conditions (temperature: $22\pm 1^\circ\text{C}$, humidity: $50\pm 10\%$). After 1 week of acclimatization, the rats were randomly divided into two groups: the control group (CON group, $n=6$) with a low-fat diet (10% kcal from fat, Research Diets D12450B, New Brunswick, NJ, USA) and the model group ($n=16$) with a high-fat diet (HFD) (60% kcal from fat, Research Diets D12492). The constituent components of the employed diets are shown as follows (Ingredient (grams in HFD; grams in LFD)): Casein (200; 200), L-cystine (3; 3), corn starch (0; 315), maltodextrin 10 (125; 35), sucrose (68; 350), cellulose BW200 (50; 50), soybean oil (25; 25), lard (245; 20), mineral mix S10026 (10; 10), di-calcium phosphate (13; 13), calcium carbonate (5.5; 5.5), potassium citrate (16.5; 16.5), vitamin mix V10001 (10; 10), choline bitartrate (2; 2) and FD&C dye #1 (blue 0.05; yellow 0.05). Compared with the CON group's average body weight (BW), a 20% rise in the HFD group was the criterion for establishing a rat model of simple obesity [20]. After 5 weeks, four rats failed to meet the pre-defined obesity criteria. These obesity-resistant rats were excluded, and the remaining 12 rats were randomly divided into the HFD ($n=6$) and EA ($n=6$) groups. To ensure experimental precision, the type of feed was kept consistent for each group throughout the modeling and treatment phases.

Animal experimental design

In the EA group, rats were securely immobilized using a custom-made fixture. For this study, the Zusanli (ST36) and Quchi (LI11) acupoints were selected for treatment [21]. The ST36 acupoints are located 5 mm below the head of the fibula, on the outer side of the knee joint. The LI11 acupoints are the depressions on the outer front side near the proximal end of the

EA improves lipid metabolism

radius. Sterile acupuncture needles were inserted to depths of approximately 7 mm and 4 mm. The electroacupuncture instrument (SDZ-III type, Suzhou Medical Supplies Factory Co., Ltd., China) was linked and adjusted to 10 Hz and 1.5 mA, utilizing a continuous wave. Each treatment session lasted 15 min, once a day, for 21 days. BWs were measured on alternate days.

After the last EA treatment, two fecal samples from each group were taken and placed in sterile cryopreservation tubes, stored in liquid nitrogen, and kept in a -80°C freezer to detect the rat gut microbiota and SCFAs. After fasting for 16 hours, the rats were sedated with 0.2 mL/100 g of 2% pentobarbital sodium in the abdominal cavity. Body length (naso-anal) was also measured. Blood samples were obtained from the abdominal aorta. Approximately 100 mg of perirenal fat was collected for subsequent proteomic analysis. Another portion of the perirenal fat and liver was immersed in 4% paraformaldehyde for fixation for hematoxylin and eosin (HE) staining observation.

HE staining

The fixed fat tissue and liver, preserved in 4% paraformaldehyde, were sliced into 5-7 μ m and underwent HE staining. This staining method was employed to observe the size of adipocytes and assess inflammatory infiltration and lipid droplets in the liver.

Serum lipid levels

Blood was collected from the abdominal aorta and centrifuged at 954 \times g for 15 min, followed by serum collection. A clinical, fully automated biochemical analyzer was utilized to quantify serum levels of total cholesterol (TC), triglyceride (TG), high-density lipoprotein cholesterol (HDL-C), and low-density lipoprotein cholesterol (LDL-C) levels.

Tandem mass tag-labeled quantitative proteomic analysis

Protein isolation and absorption: Frozen fat tissue samples were extracted and processed in SDT lysis buffer. Following protein concentration determination via a bicinchoninic acid assay, the samples were portioned into frac-

tions and stored at -80°C. Then, they underwent trypsin cleavage, and the resulting digested samples were lyophilized.

Peptide labeling and reverse-phase chromatography separation: The lyophilized samples were thoroughly mixed with 100 mM triethylammonium bicarbonate buffer, followed by a labeling reaction in 1.5 mL Eppendorf tubes. Reverse-phase chromatographic separation was performed according to the manufacturer's instructions.

Chromatographic and mass spectrometric conditions: Chromatographic conditions Samples were placed onto Acclaim PepMap RSLC C18 (Thermo Fisher, Shanghai, China). Mobile phase A contained ACN-H₂O-FA (99.9:0.1) while mobile phase B contained ACN-H₂O-FA (80:19.9:0.1). Gradient elution conditions: 0-50 min, 2%-28% B; 50-60 min, 28%-42% B; 60-65 min, 42%-90% B; 65-75 min, 90% B.

The first-level mass spectrometry (MS) resolution was set at 60,000, with an automatic gain control value of 3e6 and a maximum injection time of 50 ms. Mass spectra were acquired using full scan mode. MS/MS spectra were obtained through data-dependent acquisition in positive ion mode, utilizing a higher-energy collisional dissociation set at 32. The MS/MS resolution was established at 45,000 (AGC value: 2e5; maximum injection time: 80 ms). Dynamic exclusion duration was set to 30 s.

Database search: Data analysis was conducted using Proteome Discoverer 2.4.1.15 (Thermo Fisher, Shanghai, China).

Western blotting

We extracted adipose tissue and total protein with RIPA buffer (Beyotime, Shanghai, China). Proteins were separated on a 10% SDS-PAGE gel (BOSTER, China) and were moved to the PVDF membrane and incubated with (Fatty Acid-Binding Protein 3) Fabp3 antibody (Affinity, Changzhou, China) and (3-Hydroxy-3-Methylglutaryl-CoA Synthase 1) Hmgcs1 antibody (Affinity, China) at 4°C overnight. After three washes, the secondary goat anti-rabbit IgG-HRP antibody (LABELAD, Beijing, China) was introduced, culminating in chemiluminescent detection. Band grayscale values were ana-

lyzed using the ImageJ software for statistical analysis.

16S rRNA amplicon sequencing

According to the manufacturer's instructions, genomic DNA was extracted from fecal samples using a MagPure Soil DNA LQ Kit (Magan). The concentration and integrity of the DNA were assessed using a NanoDrop 2000 (Thermo Fisher Scientific, USA). The extracted DNA served as the template for PCR amplification of bacterial 16S rRNA genes with bar-coded primers and Takara Ex Taq (Takara). The V3-V4 variable region of the 16S rRNA gene was amplified using universal primers 343F (5'-TACGGRAGGCAG-3') and 798R (5'-AGGGGTATCTAATCCT-3') sequenced on Illumina NovaSeq 6,000 (OE Biotech Company, Shanghai, China). QIIME 2 software was utilized for analyzing α and β diversity. The differential analysis was conducted using an analysis of variance (ANOVA) statistical algorithm from the R package. Taxonomic abundance spectra were also compared using the linear discriminant analysis effect size (LEfSe) method.

Liquid chromatograph-mass spectrometer (LC-MS) analyses

The SCFA content in rat feces was determined using LC-MS. Following pretreatment steps, including grinding, purification, and enrichment, the rat fecal samples were subjected to qualitative and quantitative detection of the target metabolites. Chromatographic conditions: 1 μ L injection volume, 0.4 mL/min, mobile phase A (0.1% formic acid aqueous) and B (acetonitrile/methanol =2:1). Gradient elution: 0 min A/B (80:20), 2 min A/B (80:20), 8 min A/B (60:40), 8.1 min A/B (5:95), 9.5 min A/B (5:95), 9.6 min A/B (80:20), 10 min A/B (80:20). Mass spectrometry conditions: curtain gas pressure of 35 (psi), CAD medium, ion spray voltage of -4500 V, ion source temperature of 450°C, column temperature of 40°C, and spray gas (Gas1) and auxiliary heating gas (Gas2) pressures 50 (psi) each. Metabolite quantification was performed using the multiple reaction detection mode of triple quadrupole mass spectrometry. The initial LC-MS data underwent processing with Progenesis Q1 V2.3 (Nonlinear Dynamics, Newcastle, UK).

Statistical analyses

Data analyses were performed using SPSS 27.0 statistical software (IBM Corp., Armonk, NY, USA), with mean \pm standard deviation results. Differences between groups were assessed using a one-way ANOVA. When variances were equal, the LSD test was applied; otherwise, Dunnett's T3 analysis was used. Statistical significance was set at $P < 0.05$.

Results

Analysis of BW, Lee's index, and serum lipid levels

After EA treatment, the BW and Lee's index (Lee's index = $\sqrt[3]{\text{body weight (g)}} \times \text{nasal length (cm)}$) for rats in the HFD group were notably higher than those for rats in the CON group ($P < 0.01$). Compared to the HFD group, the EA group displayed lower BW and Lee's index results ($P < 0.05$, $P < 0.01$; **Figure 1A** and **1B**). There were no significant differences in the body length between the groups ($P > 0.05$; **Figure 1C**). The TG and TC levels were significantly higher in the HFD group compared to the CON group ($P < 0.05$). After EA intervention, there was a great reduction in TG and TC levels in the EA group compared to the HFD group ($P < 0.01$, $P < 0.05$, respectively) (**Figure 1D** and **1E**). There were no significant differences in the HDL-C or LDL-C levels between the groups ($P > 0.05$; **Figure 1F** and **1G**).

Histological examinations

Figure 2A shows that the adipocytes in the CON group were normal in size. In contrast, the HFD group showed an enlarged adipocyte diameter. Following EA treatment, adipocytes in the EA group showed a reduction in diameter. Compared to the control group, the HFD group had significant hepatocyte vacuolization, with a larger and more numerous vacuolar area accompanied by cellular steatosis and an inflammatory response. After EA treatment, there was less vacuolization of liver cells and a significant improvement in inflammatory infiltration (**Figure 2B**).

Proteomic analysis of adipose tissue in obese rats

The principal component analysis used reliable protein expression levels to depict the relation-

EA improves lipid metabolism

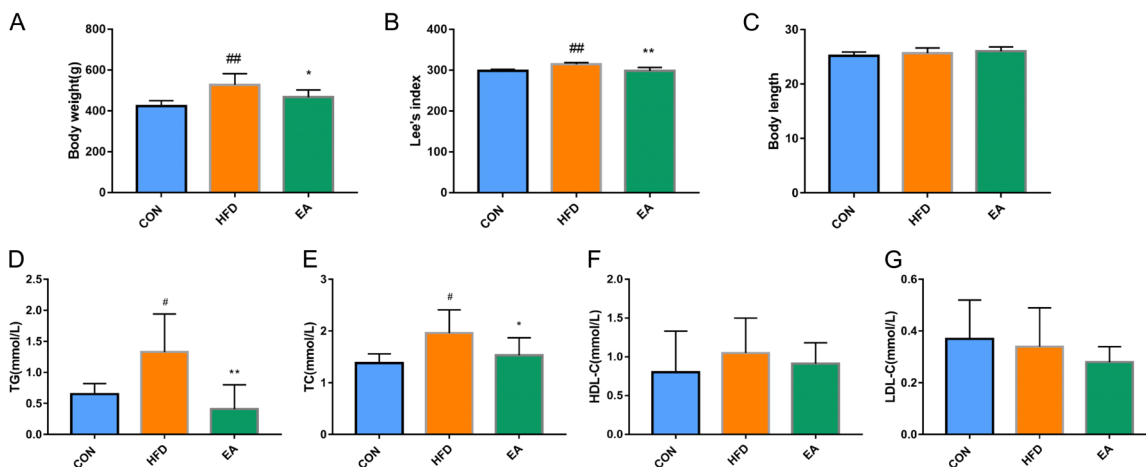


Figure 1. Effects of electroacupuncture (EA) on body weight (BW) and serum lipid levels in rats. (A) BW, (B) Lee's index, (C) Serum triglyceride (TG), (D) Serum total cholesterol (TC), (E) Serum low-density lipoprotein cholesterol (LDL-C), (F) Serum high-density lipoprotein cholesterol (HDL-C), (G) Serum low-density lipoprotein cholesterol (LDL-C). Data are presented as means \pm standard error of the mean (n=6). Statistical significance: # P <0.05 vs. control group (CON); ## P <0.01 vs. CON; * P <0.05 vs. high-fat diet (HFD); ** P <0.01 vs. HFD.

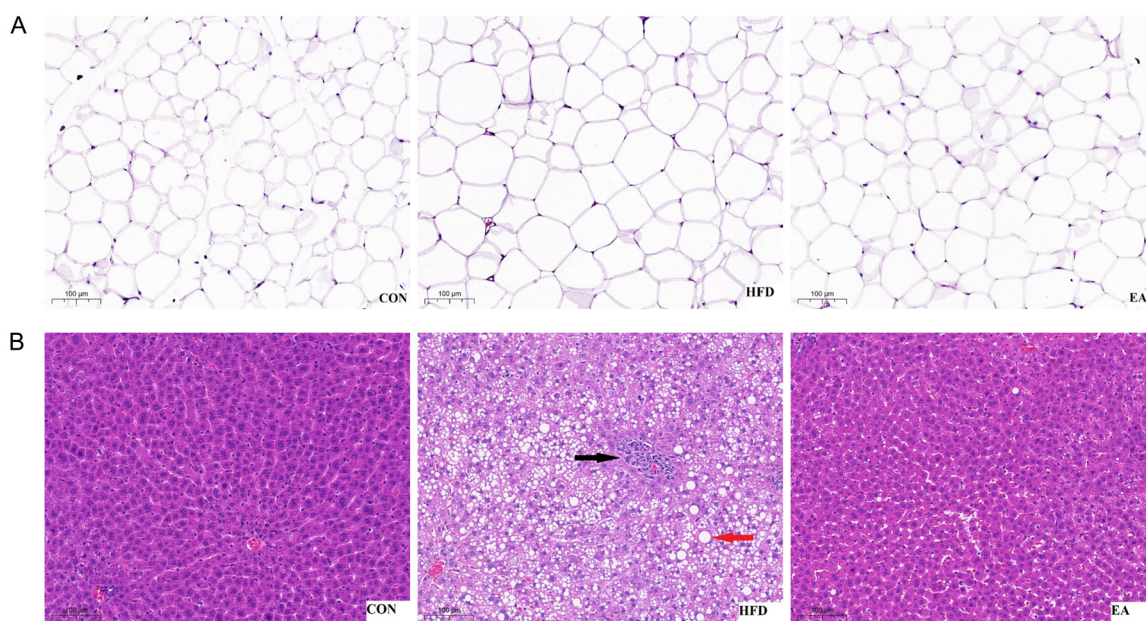


Figure 2. Histomorphological changes of adipose tissue and liver in rats of each group. Red arrows indicate lipid droplets. Black arrows indicate inflammatory infiltration. (A) Histomorphological changes of adipose tissues, (B) Liver histomorphological changes. Scale bar =100 μ m.

ships between the samples. Each data point on the graph represents a sample, with distinct colors denoting different groups. In the score plot, greater distances between data points signify notable disparities among samples, while closer proximity indicates greater similarity. As illustrated in **Figure 3A**, the samples from the CON group exhibited considerable

separation from those in the HFD group, indicating significant distinctions in modeling. However, after treatment, samples from the EA group became more similar to those from the CON group.

Compared to the CON group, the HFD group had 114 DEPs, encompassing 63 upregulated

EA improves lipid metabolism

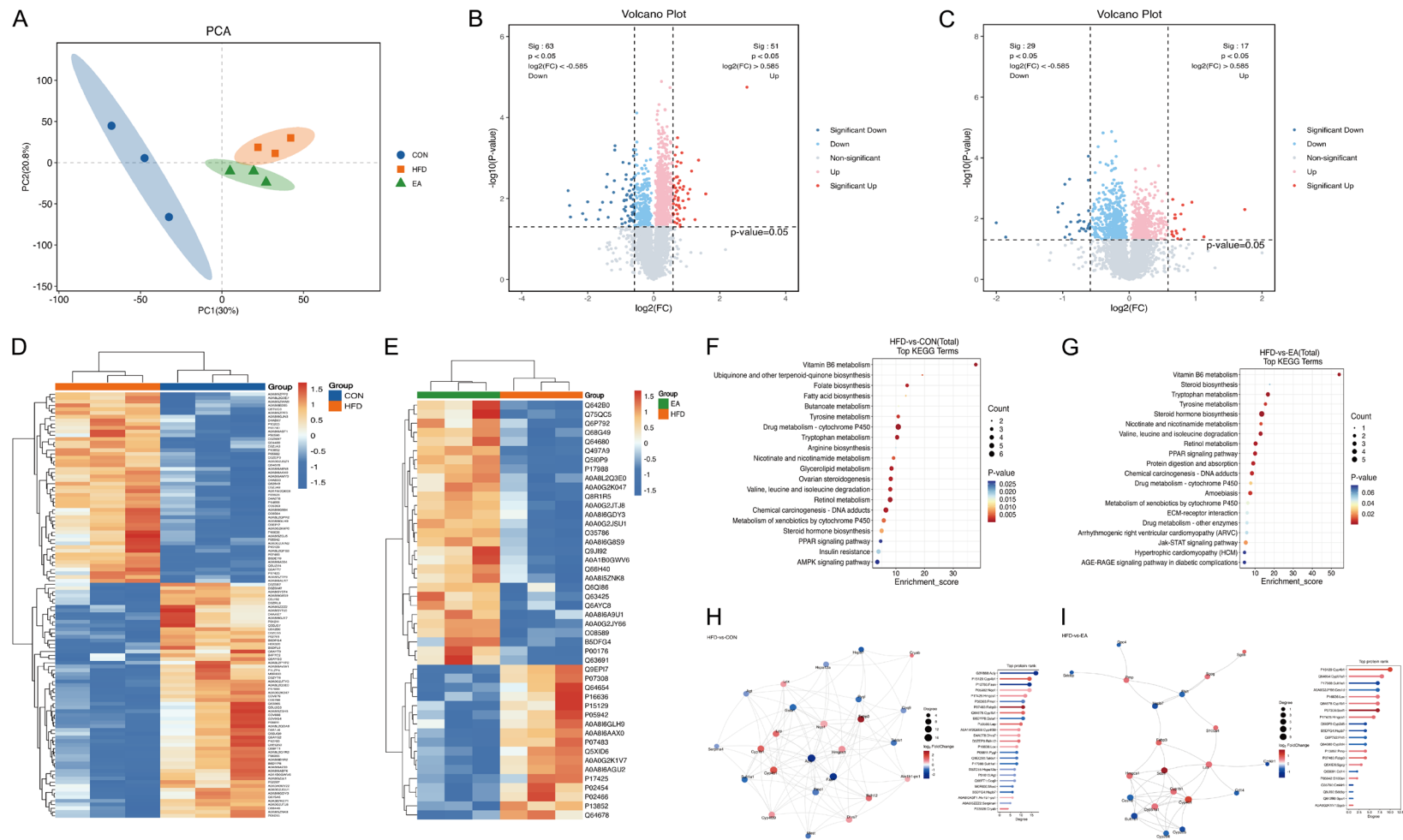


Figure 3. Analysis of differential protein expression in adipose tissue of the rats in each group. (A) Principal Component Analysis, (B) Volcano plot of high-fat diet (HFD) vs. control (CON) groups, (C) Volcano plot of HFD vs. electroacupuncture (EA), (D) Heat map of HFD vs. CON, (E) Heat map of HFD vs. EA, (F) Kyoto Encyclopedia of Genes and Genomes KEGG pathway enrichment of differentially expressed proteins (DEPs) between the HFD and CON groups, (G) KEGG pathway enrichment of DEPs between the HFD and EA group, (n=3), (H) Protein-protein Interaction (PPI) network of DEPs between HFD and CON group, and (I) PPI network of DEPs between the HFD and EA group.

EA improves lipid metabolism

Table 1. Differential protein expression in adipose tissue of rats in each group

Proteins	CON vs. HFD			HFD vs. EA		
	FC	P value	Regulation	FC	P value	Regulation
Aox2	0.858991169	0.014796053	Down	1.119580519	0.040442129	Up
Hsd11b1	0.914379717	0.023451053	Down	1.039839641	0.021409963	Up
Acss3	0.936800147	0.033132277	Down	1.0420207	0.011607412	Up
Hspb7	0.915692462	0.012086579	Down	1.067658318	0.047716352	Up
Slc36a2	0.942699097	0.032582921	Down	1.046624525	0.025336696	Up
Sult1a1	0.954701787	0.029101088	Down	1.049306796	0.000738008	Up
Zfp317	0.941206102	0.003628454	Down	1.050167926	0.02104401	Up
Slc43a3	0.954898148	0.000634448	Down	1.061836524	0.004260112	Up
Slc1a3	0.957311323	0.000495544	Down	1.061054182	0.006065219	Up
Sdcbp	0.960029014	0.031996695	Down	1.046665661	0.025576901	Up
Gpc4	0.96557975	0.003342601	Down	1.039835443	0.012487517	Up
S100a4	1.035165031	0.007941837	Up	0.961235348	0.03046787	Down
magel-D	1.04370604	0.026535686	Up	0.961640788	0.002331447	Down
Lox	1.05726117	0.001361605	Up	0.949795837	0.037714473	Down
Hmgcs1	1.045151633	0.006427626	Up	0.95946204	0.045514751	Down
Prnp	1.055574639	0.030760617	Up	0.955999965	0.007389571	Down
Gpnmb	1.064726361	0.00877475	Up	0.953909017	0.046223787	Down
Cyp1b1	1.094720223	0.009659134	Up	0.955572261	0.009578482	Down
Cyp4b1	1.083891973	0.034610667	Up	0.944861389	0.039724158	Down
Fabp3	1.150282177	0.015584069	Up	0.96267732	0.003545035	Down

Table 2. The KEGG related to obesity with differentially expressed proteins between the HFD and CON group

Pathway name	Protein ID	Number	P value
Glycerolipid metabolism	Plpp1, Akr1b1, Akr1b1-ps1, Mgll	5	0.00129058894382278
Fatty acid biosynthesis	Fasn, Acaca	2	0.009724664078492
PPAR signaling pathway	Fabp3, Hmgcs1, Plin2	3	0.0263954106616092
AMPK signaling pathway	Fasn, Acaca, Slc2a4, Lep	4	0.02691986
Insulin resistance	Agt, Pygl, Slc2a4, Slc27a3	4	0.018846067
Jak-STAT signaling pathway	Lep, Aox3, Aox2, Aox3	4	0.036797124

and 51 downregulated proteins ($P < 0.05$). Forty-six DEPs were identified in the EA group, with 29 upregulated and 17 downregulated proteins ($P < 0.05$) compared to the HFD group (**Figure 3B-E**). Quantitative comparisons of these common DEPs in all three groups are listed in **Table 1**. Among these proteins, Hmgcs1 and Fabp3 were upregulated in the HFD group. After EA intervention, the expression of these proteins was downregulated ($P < 0.05$).

The Kyoto Encyclopedia of Genes and Genomes (KEGG) analysis revealed significant alterations in the top 20 pathways due to EA therapy.

These pathways include the peroxisome proliferator-activated receptor (PPAR) signaling pathway, steroid hormone biosynthesis, vitamin B6 metabolism, tryptophan metabolism, valine, leucine and isoleucine degradation, retinol metabolism, protein digestion and absorption, and amoebiasis (**Figure 3F, 3G; Tables 2 and 3**).

A predictive analysis of the interactions between the DEPs was conducted using the Search Tool for the Retrieval of Interacting Genes/Proteins (STRING) Proteins such as Hmgcs1, Fabp3, cytochrome P450 family 51 subfamily A member 1 (Cyp51a1), sulfotrans-

EA improves lipid metabolism

Table 3. The KEGG related to obesity with differentially expressed proteins between the HFD and EA group

Pathway name	Protein ID	Number	P value
Steroid hormone biosynthesis	Cyp2b1, Cyp2d5, Hsd11b1, Cyp1b1, Cyp2d4	5	3.02E-05
PPAR signaling pathway	Scd1, Fabp3, Hmgcs1	3	0.003241738
Tryptophan metabolism	Aox3, Cyp1b1, Aox2	3	0.000746928
Jak-STAT signaling pathway	AAox3, Aox2, Fhl1	3	0.020216707
Vitamin B6 metabolism	Aox3, Aox2	2	0.000624609

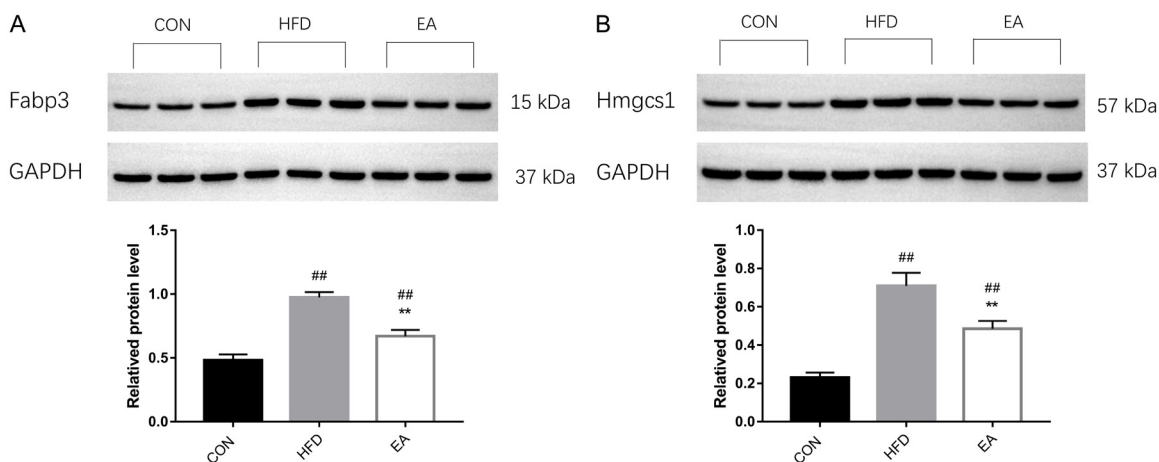


Figure 4. Verification of Fabp3 and Hmgcs 1 protein expression by western blot. ## $P < 0.01$ vs. control (CON) group. Statistical significance: ** $P < 0.01$ vs. high-fat diet (HFD) group (n=3).

ferase 1A1 (Sult1a1), carboxylesterase 1D (Ces1d), lipoxygenase (Lox), stearoyl-CoA desaturase 1 (Scd1), heat shock protein family B member 7 (Hspb7), four and a half LIM domains 1 (Fhl1), cytochrome P450 family 2 subfamily D member 4 (Cyp2d4), and prion protein (Prnp) occupied central positions in the network diagram (**Figure 3H, 3I**).

Western blot validation

A western blot analysis was performed to validate the outcomes of the KEGG pathway analysis, with a specific focus on the PPAR signaling pathway, Fabp3, and Hmgcs1. The results demonstrated a significant increase in Fabp3 and Hmgcs1 protein expression levels in the HFD group ($P < 0.01$). However, following EA intervention, the protein expressions for Fabp3 and Hmgcs1 in the EA group significantly decreased ($P < 0.01$), which was consistent with the trend observed in the proteomic analysis, underscoring their roles within the protein-protein interaction network elucidated in **Figure 4**.

Gut microbiota and SCFAs analysis of fecal samples in obese rats

The principal coordinates analysis results showed that the CON and HFD group samples were far apart, indicating a significant difference in the microbiota composition between the two groups. The microbiota profiles of the HFD and EA groups were separated to some extent (**Figure 5A**). The relative abundance and LEfSe analysis revealed that the dominant bacterial communities in the EA group included Bacteroidetes, *Blautia*, *Roseburia*, and Burkholderia. In contrast, the dominant microbial communities in the HFD group were Firmicutes, *Clostridia*, and Lachnospiraceae_NK4A136_group. The beneficial microbial communities of the CON group included *Coprococcus* and *Butyrivibrio*. Firmicutes, Bacteroidetes, *Bacteroidota*, and *Roseburia* were closely related to obesity and could be reversed by EA intervention (**Figure 5B-E**).

We examined seven major SCFAs in fecal samples post-EA treatment, noting a substantial

EA improves lipid metabolism

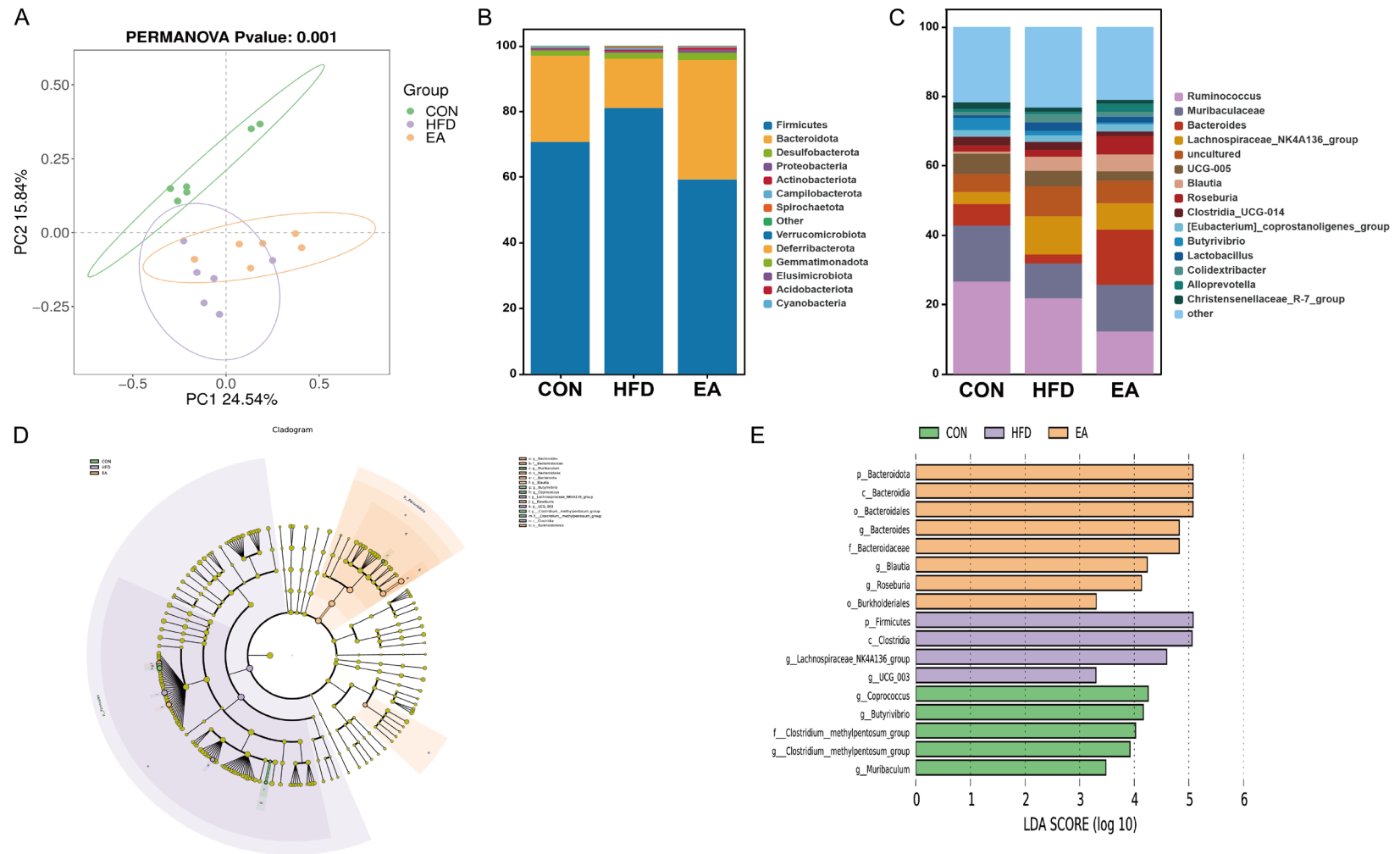


Figure 5. PCoA, relative abundance and LEfSe analyses of gut microbiota diversity. (A) PCoA analysis, (B, C) Relative abundance of phylum and genus, (D, E) LEfSe analysis.

EA improves lipid metabolism

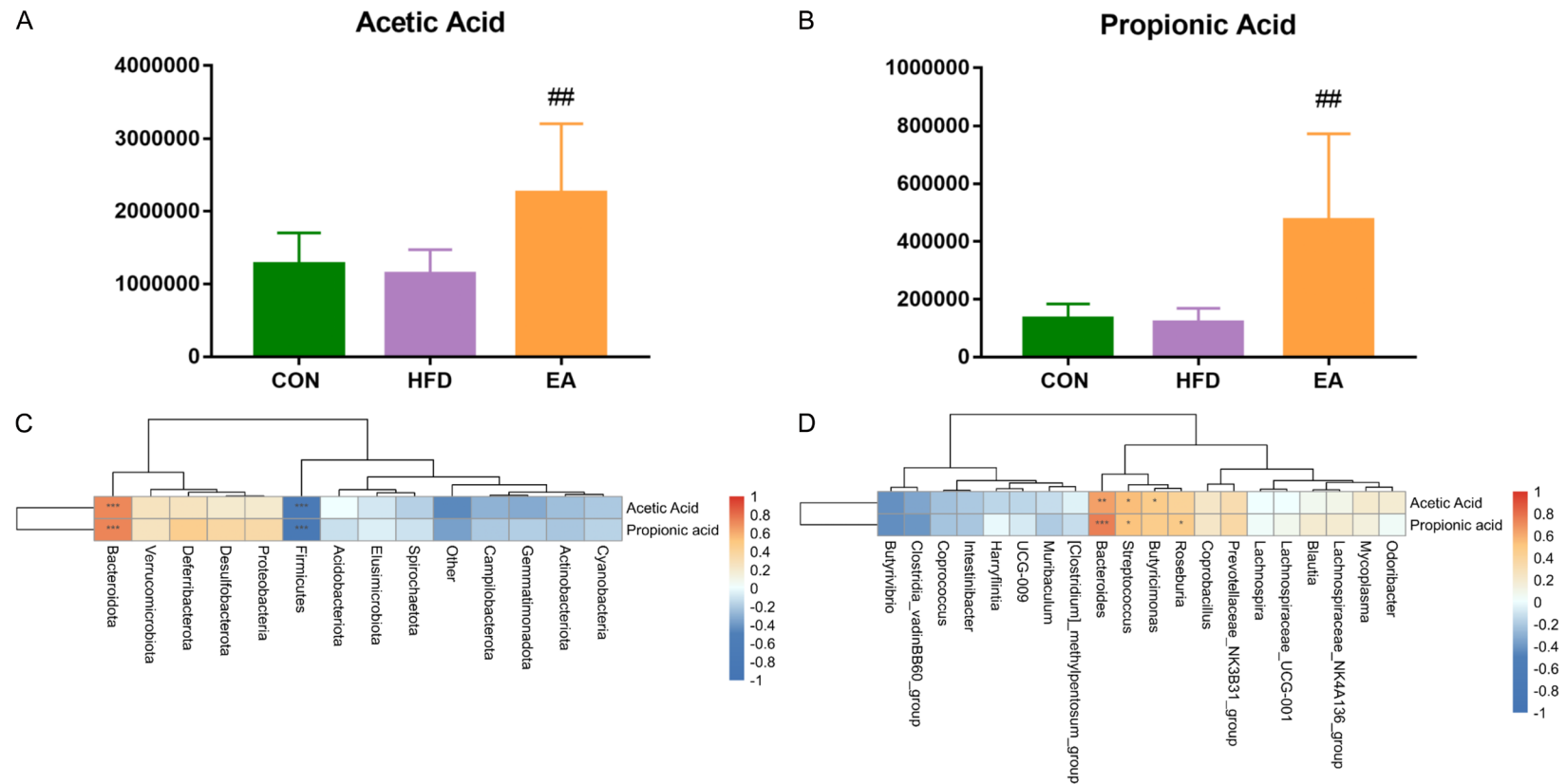


Figure 6. Short-chain fatty acids (SCFAs) production in feces and correlation analysis between gut microbiota and SCFAs. (A) Acetic acid, (B) Propionic acid. Statistical, (C) Correlation analysis between gut microbiota and SCFA at the phylum level, (D) Correlation analysis between gut microbiota and SCFA at the genus level. ^{##} $P < 0.01$ vs. high-fat diet (HFD) group.

EA improves lipid metabolism

elevation in acetic and propionic acid levels ($P < 0.01$) (Figure 6A, 6B). The Pearson correlation analysis between phylum-level and genus-level microbiota and SCFAs revealed that Bacteroidota was strongly associated with these acids at the phylum level. In contrast, Firmicutes correlated significantly negatively with acetic and propionic acid levels. At the genus level, *Bacteroides*, *Streptococcus*, and *Butyrivibrio* were positively correlated with acetic acid, whereas *Bacteroides*, *Streptococcus*, and *Roseburia* were positively correlated with propionic acid (Figure 6C, 6D).

Discussion

This study demonstrated the significant effects of EA in alleviating weight gain, blood lipid concentrations, and adiposity in both adipose and hepatic tissues. Additionally, our findings reveal that EA induced notable alterations in the gut microbiota's composition, structure, and metabolic function, particularly by enhancing the production of SCFAs. Firmicutes and Bacteroidota are predominant bacterial phyla in the human gut microbiota, collectively representing over 90% of the total community [22]. Our study revealed a decline in the abundance of Firmicutes and an elevation in Bacteroidota following EA treatment. Previous studies have determined that the gut microbiota of animals and individuals with obesity exhibits a higher Firmicutes/Bacteroidetes (F/B) ratio in contrast to non-obese counterparts, implying the potential utility of this ratio as a biomarker [23]. Maintaining a balanced intestinal ecosystem is critical for normal physiological function [24], and EA can achieve an appropriate F/B ratio. At the genus level, *Bacteroides* is a well-studied member of the gut microbiota, known for its beneficial microbiota. It participates in propionic acid production and the reduction of lipopolysaccharides synthesis [25]. Elevated lipopolysaccharide levels can induce systemic inflammation and compromise gut barrier function [26]. A decrease in the genus *Bacteroides* has been demonstrated in patients with obesity [27]. *Roseburia* contributes to weight loss through its ability to metabolize glucose to produce final products such as acetic and butyric acids [28]. Our study found that EA reduced the F/B ratio and promoted *Bacteroides* and *Roseburia* growth. These findings suggest the

anti-obesity potentials of EA in regulating the gut microbiota.

Alterations in gut microbiota composition have profound implications for producing its metabolites, particularly SCFAs, metabolites of gut microbiota that serve as important mediators of interactions between hosts and gut microbiota [29]. SCFAs, produced by the gut microbiota, mainly comprise acetic acid, propionic acid, and butyric acid, constituting 91.18% of these metabolites [30]. These three types of SCFAs can exert various physiologic effects, such as lowering intestinal pH, suppressing pathogenic bacteria proliferation, and boosting the quantity of beneficial bacteria. Furthermore, butyric and propionic acids have been reported to reduce appetite by stimulating intestinal appetite hormone release [31]. Furthermore, acetic acid may promote lipolysis and fatty acid oxidation by activating the G protein-coupled receptor 41/43 [32], adenosine monophosphate-activated protein kinase, and extracellular signal-regulated kinase 1/2 signaling pathways, and inhibiting fatty acid synthesis to inhibit lipid accumulation and reduce hepatic triglyceride content. In the liver, propionic acid can inhibit the synthesis of cholesterol and the production of new fats, reducing liver fat [33]. Our findings demonstrated that EA intervention promoted the production of acetic acid and propionic acid. In addition, the liver is the focal point of fatty acid metabolism and lipid circulation, and the accumulation of liver cell lipid droplets results from fatty acid synthesis and oxidation. In the present study, the EA group had improvements in blood lipid levels, liver inflammatory infiltration, and lipid droplets. These results suggest that EA regulates SCFAs production by affecting the intestinal microbiota composition, mediating lipid metabolism disorders, and exerting anti-obesity effects. This study also employed proteomic analysis to identify DEPs in the adipose tissue of obese rats modeled for obesity. Our comprehensive analysis of DEPs and KEGG enrichment pathways demonstrated that EA affected many obesity-related proteins, especially those within the PPAR signaling pathway. PPAR is important in regulating preadipocyte differentiation into mature adipocytes, lipid deposition in adipocytes, and mediating cholesterol efflux through various pathways in cholesterol metabolism [34]. Our find-

EA improves lipid metabolism

ings revealed that EA treatment regulates genes such as *Fabp3* and *Hmgcs1* within the PPAR signaling pathway. *Fabp3*, a member of the intracellular lipid-binding protein family, encodes a protein responsible for fatty acid transport and metabolism. It plays a pivotal role in fat synthesis, breakdown, and homeostasis [35, 36]. *Fabp3* mRNA is markedly up-regulated in hepatic and adipose tissue of rats with high-cholesterol diets [37, 38]. *Hmgcs1* is pivotal in the synthesis of cholesterol, as it reduces the synthesis of cholesterol. Consequently, the downregulation of *Hmgcs1* primarily inhibits cholesterol biosynthesis and modulates cholesterol metabolism [39]. In line with this, our study found that EA administration led to decreased adipose and hepatic fat deposition, along with reduced TC and TG plasma levels in HFD rats. These findings were corroborated by alterations observed in proteins within the PPAR signaling pathway.

The association between gut microbiota and the PPAR signaling pathway has been extensively investigated [40, 41], with some SCFA-producing gut microbiota shown to regulate the PPAR signaling pathway, thereby alleviating obesity. Acetic acid enhances adipocyte differentiation via upregulating PPAR γ gene expression in adipose tissue [42]. Our study revealed that EA increases SCFA-producing gut microbiota and the feces' levels of acetate and propionate. This finding could help elucidate the alterations observed in PPAR signaling. However, further investigations are necessary to validate this association.

In the proteomic analysis, we observed several obesity-related proteins modulated by EA, which may elucidate the mechanisms underlying EA's anti-obesity effects. Notably, *Cyp1b1*, a novel member of the CYP450 superfamily closely associated with lipid metabolism and inflammatory responses, has been implicated in macrophage recruitment and pro-inflammatory processes. Studies demonstrate that *Cyp1b1* knockout mice resist HFD-induced obesity [43], while *Cyp1b1*-mediated macrophage activation contributes to HFD-induced insulin resistance [44]. Another key regulator, *Acsc3*, is an essential mitochondrial inner membrane protein enriched in brown adipose tissue (BAT) that mediates propionate metabo-

lism. *Acsc3* deficiency induces BAT whitening, enhances adipocyte autophagy, promotes lipid accumulation, and ultimately leads to insulin resistance and systemic metabolic syndrome [45]. *Gpnmb* has been identified as a critical regulator of adipogenesis. *Gpnmb* stimulates lipogenesis in white adipose tissue, exacerbating diet-induced obesity and insulin resistance [46]. Neutralizing antibodies against *Gpnmb* effectively reverse obese phenotypes in mice by reducing adipose mass, suppressing lipogenic gene expression, promoting thermogenesis, and improving insulin sensitivity.

This study's limitations include the small sample size and all discovered DEPs were not verified using western blotting. Subsequent research will enhance the sample size and verify more signal pathway-related proteins, improving the study results' accuracy and credibility.

Conclusions

Our findings demonstrated that EA can alleviate obesity by regulating the composition of gut microbiota, including promoting beneficial bacteria growth and augmentation of SCFA levels. These mechanisms activate the PPAR signaling pathway, essential in lipid metabolism. This study provides a foundation for further investigation into the mechanisms underlying the beneficial effects of EA for obesity treatment.

Acknowledgements

This study was supported by the Natural Science Foundation of Chongqing, China (CS-TB2024NSCQ-MSX0124, cstc2021jcyj-msxm-X0485); Natural Science Research Projects of Chongqing Three Gorges Medical College (No. XJ2022003202); High Level Talent Research Launch Fund Project of Chongqing Three Gorges Medical College; Chongqing Key Laboratory of Development and Utilization of Genuine Medicinal Materials in Three Gorges Reservoir Area (No. KJZD-M202202701); and the Chongqing Talents Plan Project (No: cstc2022ycjh-bgzxm0226).

Disclosure of conflict of interest

None.

Abbreviations

EA, Electroacupuncture; CON, Control group; HFD, High-fat diet; TC, Total cholesterol; TG, Triglyceride; SCFAs, Short-chain fatty acids; LC-MS, Liquid chromatography-mass spectrometry; PPAR, Peroxisome proliferator-activated receptor; LDL-C, Low-density lipoprotein cholesterol; HDL-C, High-density lipoprotein cholesterol; DEPs, Differentially expressed proteins; PPI, Protein-protein interaction; BW, Body weight.

Address correspondence to: Dr. Xiurong Tian, Department of Traditional Chinese Medicine, Chongqing Three Gorges Medical College, No. 366, Tianxing Road, Wanzhou District, Chongqing 404120, China. E-mail: 2022140055@sdutcm.edu.cn

References

- [1] Ternák G, Németh M, Rozanovic M, Márovics G and Bogár L. “Growth-promoting effect” of antibiotic use could explain the global obesity pandemic: a European survey. *Antibiotics (Basel)* 2022; 11: 1321.
- [2] Kelly T, Yang W, Chen CS, Reynolds K and He J. Global burden of obesity in 2005 and projections to 2030. *Int J Obes (Lond)* 2008; 32: 1431-1437.
- [3] Chung CY, Yang AWH, Foe A, Li M and Lenon GB. The clinical evaluation of electroacupuncture combined with mindfulness meditation for overweight and obesity: study protocol for a randomized sham-controlled clinical trial. *Trials* 2022; 23: 818.
- [4] Qi X, Li Z, Han J, Liu W, Xia P, Cai X, Liu X, Liu X, Zhang J and Yu P. Multifaceted roles of T cells in obesity and obesity-related complications: a narrative review. *Obes Rev* 2023; 24: e13621.
- [5] Liu T, Wu B, Yao Y, Chen Y, Zhou J, Xu K, Wang N and Fu C. Associations between depression and the incident risk of obesity in southwest China: a community population prospective cohort study. *Front Public Health* 2023; 11: 1103953.
- [6] Kosmalski M, Deska K, Bąk B, Różycka-Kosmalska M and Pietras T. Pharmacological support for the treatment of obesity-present and future. *Healthcare (Basel)* 2023; 11: 433.
- [7] Singh AK and Singh R. Pharmacotherapy in obesity: a systematic review and meta-analysis of randomized controlled trials of anti-obesity drugs. *Expert Rev Clin Pharmacol* 2020; 13: 53-64.
- [8] Neovius M, Bruze G, Jacobson P, Sjöholm K, Johansson K, Granath F, Sundström J, Näslund I, Marcus C, Ottosson J, Peltonen M and Carlsson LMS. Risk of suicide and non-fatal self-harm after bariatric surgery: results from two matched cohort studies. *Lancet Diabetes Endocrinol* 2018; 6: 197-207.
- [9] Chang SH, Freeman NLB, Lee JA, Stoll CRT, Calhoun AJ, Eagon JC and Colditz GA. Early major complications after bariatric surgery in the USA, 2003-2014: a systematic review and meta-analysis. *Obes Rev* 2018; 19: 529-537.
- [10] Yin Y, Zhao Q, Li S, Jiang H, Yin C, Chen H and Zhang Y. Efficacy of acupuncture and moxibustion therapy for simple obesity in adults: a meta-analysis of randomized controlled trials. *Medicine (Baltimore)* 2022; 101: e31148.
- [11] Wang JJ, Huang W, Wei D, Yang TY and Zhou ZY. Comparison of therapeutic effects of electroacupuncture and acupoint catgut embedding in reducing serum leptin and insulin levels in simple obesity patients. *Zhen Ci Yan Jiu* 2019; 44: 57-61.
- [12] Chen X, Huang W, Jin Y, Hu F, Cheng X, Hong Z and Zhou Z. Prescription analysis of electroacupuncture for simple obesity based on complex network technique. *Zhongguo Zhen Jiu* 2018; 38: 331-336.
- [13] Ley RE, Bäckhed F, Turnbaugh P, Lozupone CA, Knight RD and Gordon JI. Obesity alters gut microbial ecology. *Proc Natl Acad Sci U S A* 2005; 102: 11070-11075.
- [14] Alshairi NA. The role of short-chain fatty acids in mediating very low-calorie ketogenic diet-infant gut microbiota relationships and its therapeutic potential in obesity. *Nutrients* 2021; 13: 3702.
- [15] Liu X, He JF, Qu YT, Liu ZJ, Pu QY, Guo ST, Du J and Jiang PF. Electroacupuncture improves insulin resistance by reducing neuroprotein Y/agouti-related protein levels and inhibiting expression of protein tyrosine phosphatase 1B in diet-induced obese rats. *J Acupunct Meridian Stud* 2016; 9: 58-64.
- [16] Tian HR, Zhou YD, Lu DM, Yang SR, Kang WW, Tang Q and Liang FX. Effects of electroacupuncture on the inflammatory response and intestinal flora in obese rats. *Zhen Ci Yan Jiu* 2024; 49: 949-956.
- [17] McArdle AJ and Menikou S. What is proteomics? *Arch Dis Child Educ Pract Ed* 2021; 106: 178-181.
- [18] Révész Á, Hevér H, Steckel A, Schlosser G, Szabó D, Vékey K and Drahos L. Collision energies: optimization strategies for bottom-up proteomics. *Mass Spectrom Rev* 2023; 42: 1261-1299.
- [19] Tang W, Dong M, Teng F, Cui J, Zhu X, Wang W, Wuniquiemu T, Qin J, Yi L, Wang S, Dong J and Wei Y. TMT-based quantitative proteomics reveals suppression of SLC3A2 and ATP1A3 ex-

EA improves lipid metabolism

- pression contributes to the inhibitory role of acupuncture on airway inflammation in an OVA-induced mouse asthma model. *Biomed Pharmacother* 2021; 134: 111001.
- [20] Zhou YD, Yang SR, Wang YY, Lu W, Chen L and Liang FX. Effect of electroacupuncture at different acupoint combination on intestinal inflammatory response and intestinal flora in obese rats. *Zhongguo Zhen Jiu* 2022; 42: 1145-1152.
- [21] Expert Group of the “Clinical Guidelines for Traditional Chinese Medicine Weight Management” of the China Association of Chinese Medicine and the Obesity Specialty Alliance of the Guangdong Provincial Acupuncture Society. Expert Consensus on the Diagnosis and Treatment of Obesity with Traditional Chinese Medicine. *Journal of Beijing University of Traditional Chinese Medicine* 2022; 45: 9.
- [22] Wang JJ, Zhuang PF, Lin B, Li HQ, Zheng JL, Tang WL, Ye WB, Chen XJ and Zheng MP. Gut microbiota profiling in obese children from Southeastern China. *Bmc Pediatrics* 2024; 24: 193.
- [23] Fabien M, Martin G, Lea G, Alejandra Z, Susana P, Paola N and Ramadass B. The firmicutes/bacteroidetes ratio: a relevant marker of gut dysbiosis in obese patients? *Nutrients* 2020; 12: 1474.
- [24] Spase S, Aleš B and Borut Š. The influence of probiotics on the firmicutes/bacteroidetes ratio in the treatment of obesity and inflammatory bowel disease. *Microorganisms* 2020; 8: 1715.
- [25] Yue SJ, Wang WX, Zhang L, Liu J, Feng WW, Gao H, Tang YP and Yan D. Anti-obesity and gut microbiota modulation effect of astragalus polysaccharides combined with berberine on high-fat diet-fed obese mice. *Chin J Integr Med* 2023; 29: 617-625.
- [26] Tilg H, Zmora N, Adolph TE and Elinav E. The intestinal microbiota fuelling metabolic inflammation. *Nat Rev Immunol* 2020; 20: 40-54.
- [27] Song MY, Wang JH, Eom T and Kim H. *Schisandra chinensis* fruit modulates the gut microbiota composition in association with metabolic markers in obese women: a randomized, double-blind placebo-controlled study. *Nutr Res* 2015; 35: 655-663.
- [28] Fu JY, Bonder MJ, Cenit MC, Tigchelaar EF, Maatman A, Dekens JAM, Brandsma E, Marczyńska J, Imhann F, Weersma RK, Franke L, Poon TW, Xavier RJ, Gevers D, Hofker MH, Wijmenga C and Zhernakova A. The gut microbiome contributes to a substantial proportion of the variation in blood lipids. *Circ Res* 2015; 117: 817-824.
- [29] Wilkins AT and Reimer RA. Obesity, early life gut microbiota, and antibiotics. *Microorganisms* 2021; 9: 413.
- [30] Wang GZ, Sun CY, Xie BJ, Wang T, Liu HW, Chen XL, Huang QJ, Zhang CH, Li TH and Deng WQ. *Cordyceps guangdongensis* lipid-lowering formula alleviates fat and lipid accumulation by modulating gut microbiota and short-chain fatty acids in high-fat diet mice. *Front Nutr* 2022; 9: 1038740.
- [31] Lin HV, Frassetto A, Kowalik EJ, Nawrocki AR, Lu MFM, Kosinski JR, Hubert JA, Szeto D, Yao XR, Forrest G and Marsh DJ. Butyrate and propionate protect against diet-induced obesity and regulate gut hormones via free fatty acid receptor 3-independent mechanisms. *PLoS One* 2012; 7: e35240.
- [32] He G, Chen TC, Huang LF, Zhang YY, Feng YJ, Liu QJ, Yin XJ, Qu SK, Yang C, Wan JH, Liang L, Yan J and Liu W. Tibetan tea reduces obesity brought on by a high-fat diet and modulates gut flora in mice. *Food Sci Nutr* 2023; 11: 6582-6595.
- [33] Liu M, Wang WJ, Lv QY, Xiao J, Xu QS and Jiao SR. Tea polyphenols combined with *Lactobacillus rhamnosus* R5 ameliorate obesity, and alter gut microbiota composition in high-fat-diet-fed mice. *International Food Research Journal* 2024; 31: 203-214.
- [34] Yang NF, Wang YX, Tian Q, Wang QP, Lu Y, Sun LC, Wang SJ, Bei YC, Ji JG, Zhou H, Yang W, Yao PJ, Zhu WY, Sun LY, Huang ZF, Li XK and Shen PP. Blockage of PPAR γ T166 phosphorylation enhances the inducibility of beige adipocytes and improves metabolic dysfunctions. *Cell Death Differ* 2023; 30: 766-778.
- [35] Dulewicz M, Kulczyńska-Przybik A, Słowik A, Borawska R and Mroczo B. Fatty acid binding protein 3 (FABP3) and apolipoprotein E4 (ApoE4) as lipid metabolism-related biomarkers of Alzheimer's disease. *J Clin Med* 2021; 10: 3009.
- [36] Shimada Y, Kuninaga S, Ariyoshi M, Zhang B, Shiina Y, Takahashi Y, Umemoto N, Nishimura Y, Enari H and Tanaka T. E2F8 promotes hepatic steatosis through FABP3 expression in diet-induced obesity in zebrafish. *Nutr Metab (Lond)* 2015; 12: 17.
- [37] Matsuda A, Wang Z, Takahashi S, Tokuda T, Miura N and Hasegawa J. Upregulation of mRNA of retinoid binding protein and fatty acid binding protein by cholesterol enriched-diet and effect of ginger on lipid metabolism. *Life Sci* 2009; 84: 903-907.
- [38] Wang X, Hasegawa J, Kitamura Y, Wang Z, Matsuda A, Shinoda W, Miura N and Kimura K. Effects of hesperidin on the progression of hypercholesterolemia and fatty liver induced by

EA improves lipid metabolism

- high-cholesterol diet in rats. *J Pharmacol Sci* 2011; 117: 129-138.
- [39] Xiao MY, Li FF, Xie P, Qi YS, Xie JB, Pei WJ, Luo HT, Guo M, Gu YL and Piao XL. Gypenosides suppress hepatocellular carcinoma cells by blocking cholesterol biosynthesis through inhibition of MVA pathway enzyme HMGCS1. *Chem Biol Interact* 2023; 383: 110674.
- [40] Li YJ, Feng Z, Wu TL, You HX, Wang W, Liu XB and Ding L. Quinoa peptides alleviate obesity in mice induced by a high-fat diet via regulating of the PPAR- α/γ signaling pathway and gut microbiota. *Mol Nutr Food Res* 2023; 67: e2300258.
- [41] Xiao Y, Yang DM, Zhang HR, Guo H, Liao Y, Lian CH, Yao YQ, Gao H and Huang YA. Theabrownin as a potential prebiotic compound regulates lipid metabolism via the gut microbiota, microbiota-derived metabolites, and hepatic FoxO/PPAR signaling pathways. *J Agric Food Chem* 2024; 72: 8506-8520.
- [42] Liu L, Fu CY and Li FC. Acetate affects the process of lipid metabolism in rabbit liver, skeletal muscle and adipose tissue. *Animals (Basel)* 2019; 9: 799.
- [43] Li F, Jiang C, Larsen MC, Bushkofsky J, Krausz KW, Wang T, Jefcoate CR and Gonzalez FJ. Lipidomics reveals a link between CYP1B1 and SCD1 in promoting obesity. *J Proteome Res* 2014; 13: 2679-2687.
- [44] Zhao L, Liu X, Feng J, Jefcoate CR and Wang S. The role of CYP1B1 in macrophage infiltration and tissue inflammation in adult obese mice. *Acta Nutrimenta Sinica* 2012; 34: 242-249.
- [45] Jia Z, Chen X, Chen J, Zhang L, Oprescu SN, Luo N, Xiong Y, Yue F and Kuang S. ACS3 in brown fat drives propionate catabolism and its deficiency leads to autophagy and systemic metabolic dysfunction. *Clin Transl Med* 2022; 12: e665.
- [46] Gong XM, Li YF, Luo J, Wang JQ, Wei J, Wang JQ, Xiao T, Xie C, Hong J, Ning G, Shi XJ, Li BL, Qi W and Song BL. Gpnmb secreted from liver promotes lipogenesis in white adipose tissue and aggravates obesity and insulin resistance. *Nat Metab* 2019; 1: 570-583.